Heliyon 10 (2024) e38086

Contents lists available at ScienceDirect

Heliyon

journal homepage: www.cell.com/heliyon

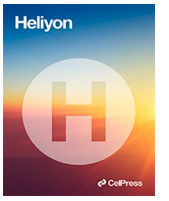

Research article

Molecular simulation of liquid-liquid extraction of acetic acid and acetone from water in the presence of nanoparticles based on prediction of solubility parameters

Hojatollah Moradi, Hossein Bahmanyar *, Hedayat Azizpour **

Surface Phenomenon and Liquid-Liquid Extraction Research Laboratory, School of Chemical Engineering, College of Engineering, University of Tehran, Tehran, Iran

ARTICLE INFO

Keywords:
Liquid-liquid extraction
Molecular dynamics simulation
Acetone
Acetic acid
Solubility parameter
Force field
Solvent

ABSTRACT

In this work, molecular dynamics simulation (MD) was used for studying the liquid-liquid extraction of acetic acid and acetone from water in the presence of nanoparticles. In the next step, the solubility parameter of acetic acid and acetone were predicted at 1 atm and different temperatures along with the solubility parameter of solvents and water at 25 °C and 1 atm. Three pure systems and three systems with different concentration of nanoparticles were investigated to show the effect of cell size or number of molecules on the solubility parameter. With the addition of SiO_2 nanoparticles to the solvents, at low concentrations of nanoparticles (0.01–0.1 vol%), the solubility parameter is increased due to the Brownian motion. With the further increase concentration of the nanoparticles, the solubility parameter decreases due to the accumulation of nanoparticles. The difference between the solubility parameter of benzene and acetone was 0.414 $(J/cm^3)^{0.5}$ and 3.13 $(J/cm^3)^{0.5}$, with and without the presence of SiO_2 nanoparticles, respectively. Finally, toluene was found to be the best solvent for acetone and acetic acid at silica nanoparticles concentration of 0.062 vol%.

1. Introduction

Acetic acid is produced in the textile, medicine, dye, and other industries and enters the environment through wastewater. The recovery of acetic acid from waste water causes savings and also prevents environmental pollution [1]. Also, acetone is widely used in chemical synthesis, especially in pharmaceutical industry. Due to its low boiling point and high volatility, acetone has many risks to human health and the environment [2]. However, when the concentration of acetic acid and acetone is very low, their recovery is very difficult. For the extraction of acetic acid and acetone, separation methods including membrane technology, absorption, extraction, distillation can be used [3], and the use of extraction and distillation methods are the most used.

Liquid-liquid extraction is a classic approach, which has a lot of applications for treatment and recycling of compounds in chemical, pharmaceutical, environmental, and oil industries [4]. Liquid-liquid extraction is selected when other methods of separation such as distillation, evaporation, and crystallization cannot be used due to the close boiling points of the compounds, inseparable mixtures, and sensitivity to high temperatures [5,6]. In the liquid-liquid extraction, selection of a proper solvent is of great importance. The

* Corresponding author.
** Corresponding author.
E-mail addresses: hbahmany@ut.ac.ir (H. Bahmanyar), h.azizpour@ut.ac.ir (H. Azizpour).

https://doi.org/10.1016/j.heliyon.2024.e38086
Received 3 June 2024; Received in revised form 13 September 2024; Accepted 17 September 2024
Available online 25 September 2024

equilibrium state between the aqueous and organic phases is one of the important aspects of the liquid-liquid extraction and in general, parameters such as physical properties (the density difference between the liquid phases and boiling point), chemical properties (distribution factor, selectivity, flammability), cost and availability are taken into account for the process design [7,8].

Moreover, addition of salts, surfactants, and nanoparticles, has a considerable impact on the hydrodynamic and mass transfer performance because of their influence on the amalgamation of the droplets and their resistance towards breakage. Surfactants reduce the interface tension considerably and are usually used to stabilize the emulsion [9]. Nanoparticles are adsorbed at the interface of the two immiscible phases and make it harder for the dispersed phase particles to coagulate by creating a spatial barrier [5]. The exact mechanism of mass transfer in nanofluids is yet not fully known. Apart from Brownian motion of particles, other mechanisms for mass transport in nanofluids are distribution stability, and aggregation. Dispersed nanoparticles aggregate and create larger particles (agglomerate), which may deposit due to the gravity. If the size of particles increases, the motion of particles becomes slower and the chance of aggregation increases [10]. Various mechanisms such as Brownian diffusion, thermophoresis, and diffusiophoresis are accountable for heat and mass transport increase [11], but according to the studies, Brownian motion of nanoparticles is the main reason of heat [12] and mass [13] transfer increase in nanofluids.

In liquid-liquid extraction systems, the solubility parameter can be used to select a suitable solvent. Solubility parameter was proposed by Hildebrand [14] and was further developed by Scatchard [15]. Hildebrand solubility parameter (HSP) is a numerical estimation of non-bonded interactions between the constituent molecules of the material [16]. Hansen [17] divided the Hildebrand parameter into three categories of polar, dispersion, and hydrogen bond, which is known as three-dimensional solubility parameter. HSP can predict the properties of mixtures such as polymer-solvent and polymer mixtures and is also useful for the selection of proper solvent and additives [16].

The solubility parameter could be measured in experiment or be calculated using experimental correlations or molecular simulation methods. However, there are limited number of correlations for calculation of HSP and cohesive energy density (CED) and furthermore, performing experiments at varying temperatures and for different solvents is time-consuming and costly. Consequently, for lack of aforementioned issues and for reliability of its results, molecular dynamics simulation has attracted researcher's attention in the past two decades [16,18–20]. Molecular dynamics simulation has been extensively used for calculating of diffusion coefficient, solubility parameter and adsorption isotherm [21–27]. Zhang et al. [28] investigated solubility parameter calculation of supercritical CO_2 (SC-CO_2) solvent and supercritical CO_2 cosolvent using molecular dynamics simulation. In a research study carried out by Li et al. [16], solubility parameter of thermoset polymers were predicted using molecular dynamic simulation. In another study done by Du et al. [29] on the solubility parameter of the supercritical carbon dioxide, it was found that increasing pressure and decreasing temperature reduces the distance between CO_2 molecules, which in turn increases the interactions between molecules and increases the solubility parameter of supercritical CO_2.

In this study, to validate the results of the molecular dynamics simulation, first the solubility parameter of the acetone and pure acetic acid were predicted using different force fields and the results were compared with the experimental data. Next, using the selected force field, solubility parameter of pure water, benzene, toluene, n-butyl acetate, carbon tetrachloride, and n-butanol were estimated and were compared with the experimental data. The effect of temperature on the solubility parameter of acetone and acetic acid was also studied by running the simulation at different temperatures. To evaluate the effect of the simulation box size or total number of molecules, solubility parameter of carbon tetrachloride was determined at two cases of with and without silica nanoparticles. Then the effect of silica nanoparticles in benzene, toluene, n-butyl acetate, carbon tetrachloride, and n-butanol solvents was studied by molecular dynamics simulation. At the end, the plot of relative concentration difference of the binary mixture at amorphous cell z direction was drawn to confirm the obtained results from the solubility parameter.

2. Theory and simulation of solubility parameter

2.1. Solubility parameter theory

Solubility parameter can be viewed as a great benchmark for selection of the solvent with best performance [30,31]. When the solubility parameter of the solvent and solute are close to each other, the solute can be dissolved in the solvent. Substances with similar values of solubility parameter are thermodynamically miscible since the non-bonded interaction energies are balanced when mixing happens [32]. There are various experimental and theoretical methods for estimation of the solubility parameter. Experimental methods for determination of solubility parameter can be divided into direct and indirect methods [32]. In the direct method, latent heat of vaporization is measured using a calorimeter and then the solubility parameter is calculated with the Hildebrand relation. In the indirect methods, the solubility parameter can be estimated using inverse gas chromatography, from melting temperatures, and intrinsic viscosity measurement [30,31].

Solubility parameter can also be estimated using theoretical methods such as PC-SAFT model, non-random hydrogen bonding, regular solution theory, and lattice energy model [33–36]. However, determination of solubility parameter from some of these methods require parameters, which are obtained from experiments and are difficult to calculate. Molecular dynamic simulation, on the other hand, is one of the methods for prediction of solvent properties, which does not rely on experimental data [37].

Hildebrand and Scott [38] defined the solubility parameter as a function of square root of the cohesive energy density. Cohesive energy (E) is the energy required to break the interactions between molecules. The relation between Hildebrand solubility parameter, molar vaporization energy (E) and molar volume (Vm) is given in Eq. (1):

$$\delta = \left(\frac{\Delta H_v - RT}{V_m}\right)^{1/2} = \sqrt{\frac{E}{V_m}} \quad (1)$$

Where ΔH_v is the enthalpy of vaporization, R is the universal gas constant, and T is the temperature. Hansen solubility parameter, as shown in Eq. (2), is comprised of three parameters of dispersion solubility (δ_d), polar solubility (δ_p), and hydrogen bond (δ_h) solubility parameters [39].

$$\delta_t^2 = \delta_d^2 + \delta_p^2 + \delta_h^2 \quad (2)$$

Where δ_d is the solubility parameter of dispersion, δ_p is the solubility parameter of polar bonds, and δ_h is the solubility parameter related to the energy of hydrogen bonds. The difference between total solubility parameters of two compounds ($\Delta\delta_t$) is often used to evaluate the miscibility of solute and solvent [40]. Greenhalgh et al. [41] showed that mixtures with $\Delta\delta < 7\ (MPa)^{0\bullet5}$ are very likely to be miscible, whereas systems with $\Delta\delta > 10\ (MPa)^{0\bullet5}$ are immiscible. Furthermore, Forster et al. [42] demonstrated that mixtures with $\Delta\delta < 2\ (MPa)^{0\bullet5}$ are miscible.

In molecular dynamics simulation, three different solubility parameters are calculated. As shown in Eq. (3), they are Hildebrand [14] solubility parameter, solubility parameter representing electrostatic forces (δ_{EL}), and another parameter representing van der Waals forces (δ_d):

$$\delta_t^2 = \delta_{EL}^2 + \delta_d^2 \quad (3)$$

δ_{EL} component is related to the hydrophilicity of the molecules, whereas the δ_d is the representative of non-polar intermolecular interactions [43].

Solubility parameter of dispersion and electrostatic forces is calculated using molecular dynamics simulation. Solubility parameter of electrostatic forces is consisted of polar and bonded forces [43,44], which is given by Eq. (4):

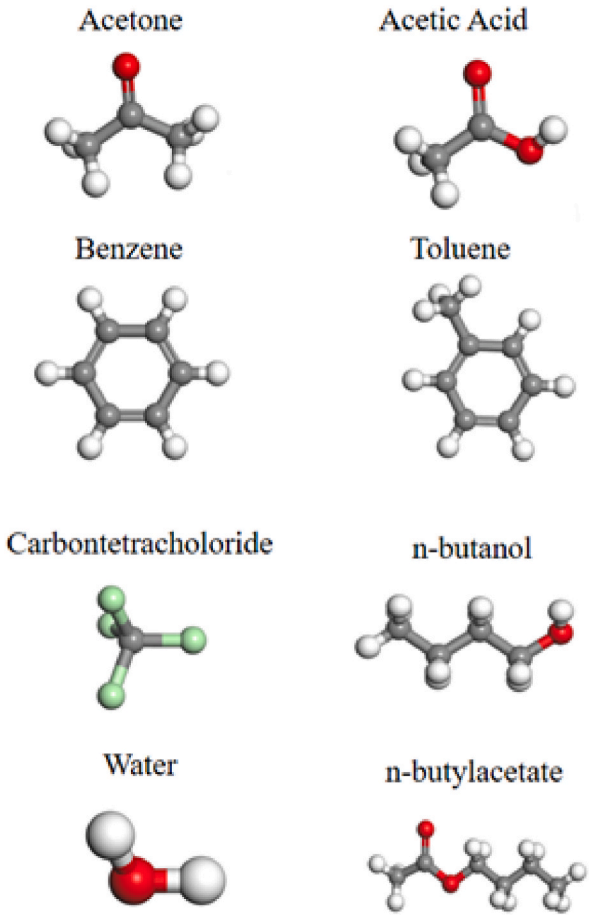

Fig. 1. Chemical structure of the molecules used in the molecular dynamic's simulation. O (red), C (grey), H (white), Cl (green). (For interpretation of the references to colour in this figure legend, the reader is referred to the Web version of this article.)

$$\delta_{EL}^2 = \delta_p^2 + \delta_h^2 \quad (4)$$

2.2. Solubility parameter simulation

In this study, all the simulations for the calculation of solubility parameter were carried out in BIOVIA Materials Studio 2017 (17.1.0.48). The three-dimensional structure of molecules in the molecular dynamic simulation is shown in Fig. 1. Canonical ensemble (NVT) and isothermal-isobaric ensemble (NPT) were used for the calculation of cohesion energy density and solubility parameters of acetic acid, acetone, toluene, benzene, n-butyl acetate, n-butanol, carbon tetrachloride, and water [18]. All the simulations were run at 298 K and pressure of 1 atm. 500 molecules were used in the amorphous cell for calculation of solubility parameter of each compound. The arrangement of the inserted molecules was first optimized by Forcite module and COMPASS force field to give the most stable structure and then the optimized structure was used to construct the amorphous cell of the simulation [45]. The amorphous cell of acetone (Fig. 2-a) and acetic acid (Fig. 2-b) at 298 K and 1 atm is depicted in Fig. 2. Ewald summation method with precision of 0.01 kcal/mol and atom-based method [18] were used to calculate van der Waals interactions with cut-off distance of 12.5 Å. The time required for NVT canonical and NPT ensemble simulations to reach equilibrium was considered 30 ps with timesteps of 1 fs [29]. Velocity scale and Berendsen barostat were used in all the simulations for calculation of the solubility parameter [28].

3. Results and discussion

3.1. Calculation of solubility parameter of pure compounds

In this work, to validate the results of the simulation, solubility parameter of acetone was calculated at 298 K and 1 atm using COMPASS, Universal, Dreiding, Cvff force fields and the outcomes were compared with the existing experimental data [46]. Table 1 shows the calculated solubility parameters of acetic acid and acetone, the measured values, and the error of simulation for each of them. As can be seen in Table 1, COMPASS force field has the lowest error with the error of 0.92 % for acetic acid and 1.81 % for acetone. Consequently, COMPASS force field was used for all the following simulations.

Calculated solubility parameter of other pure compounds at 298 K and 1 atm from molecular dynamic simulation is given in Table 2. The values of experimental data [46] for these compounds are also shown in Table 2. As can be seen, the predicted solubility parameters have a good accuracy, and the total average error of solubility parameters is 2.18 %.

Temperature and pressure are both important operating parameters in the extraction process for controlling the solubility parameter [28]. Solubility parameter of acetic acid and acetone were predicted at 1 atm and temperatures of 293, 298, 303, 308, and 313 K using molecular dynamics simulation, which are shown in Fig. 3. As can be seen in the figure, by increasing the temperature, the solubility parameter of acetic acid and acetone and also the slope of the curve are decreased. This decreasing is caused by both the effects of lower adhesion energy and lower mass density, but the former has the more prominent effect [16]. As a result, it can be concluded that the temperature decrease is favorable to the solubility parameter.

3.2. Effect of silica nanoparticles on solubility parameter

Many studies have focused on improving the performance of liquid-liquid extraction using SiO_2 nanoparticles [5,47–49]. In most of these studies, silica nanoparticles have been used with the concentration range of 0.01–0.1 vol%. In high concentrations of silica, mass transfer is reduced due to the aggregation of nanoparticles and decrease of free volume. In low concentrations, however; presence of nanoparticles would increase the mass transfer due to Brownian motion. Main advantages of using silica nanoparticles are low density,

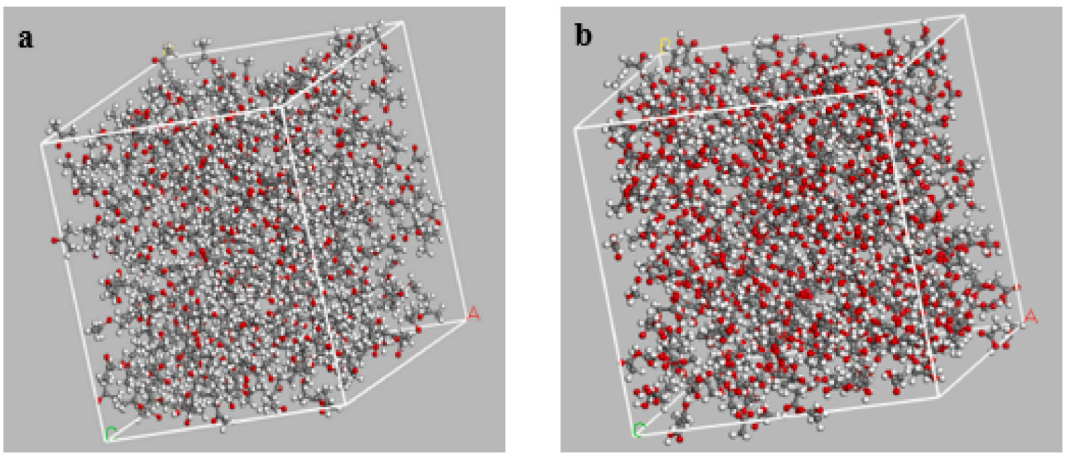

Fig. 2. Amorphous cell a) acetone b) acetic acid at 298 K and 1 atm.

Table 1
Comparison of the accuracy of different force fields for calculation of solubility parameter of acetone and acetic acid at 298 K and 1 atm.

Force field	$\delta_{t,Acetone}^{sim}$ $(J/cm^3)^{0.5}$	$\left[\frac{\lvert\delta_t^{exp}-\delta_t^{sim}\rvert}{\delta_t^{exp}}\right]^{Acetone}\times 100$	$\delta_{t,Acetic\ Acid}^{sim}$ $(J/cm^3)^{0.5}$	$\left[\frac{\lvert\delta_t^{exp}-\delta_t^{sim}\rvert}{\delta_t^{exp}}\right]^{AA}\times 100$
Dreiding	18.131	9.35	26.818	25.3
Universal	21.920	9.60	23.157	8.21
Cvff	22.255	11.3	22.951	7.25
COMPASS	20.362	1.81	21.203	0.92

Table 2
Prediction of pure compounds solubility parameter at 298 K and 1 atm.

Component	δ_t^{exp} $(J/cm^3)^{0.5}$ [46]	δ_t^{sim} $(J/cm^3)^{0.5}$	$\left[\frac{\lvert\delta_t^{exp}-\delta_t^{sim}\rvert}{\delta_t^{exp}}\right]\times 100$
Acetone	20	20.362	1.81
Toluene	18.2	18.556	1.96
Benzene	18.6	18.073	2.83
n-butyl acetate	17.4	18.549	6.60
Carbontetracholoride	17.8	17.916	0.65
Acetic acid	21.4	21.203	0.92
n-butanol	23.1	22.804	1.28
water	47.8	47.148	1.36

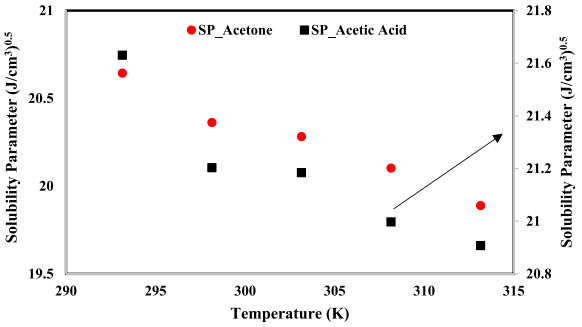

Fig. 3. Variation of acetic acid and acetone solubility parameter with respect to temperature at 1 atm.

lower particle size compared to other nanoparticles, affordable cost, variety of size, environmental compatibility, and being chemically/physically neutral expect with some specific compounds. Moreover, unique structural and performance properties of silica nanoparticles has made it one of the most popular nanoparticles in use [50].

In Tables 3–5, solubility parameters of toluene, benzene, carbon tetrachloride, n-butanol, and n-butyl acetate with presence of silica nanoparticles at various concentrations has been derived using molecular dynamic simulation. For solvents with nanoparticle concentration up to 0.1 vol%, one molecule of silica was used in the amorphous cell. Also, for concentrations of zero and 3 wt%, 500 molecules were used (sum of solvent and nanoparticle molecules). In Tables 3–5 the difference between the solubility parameter of acetic acid and acetone, with and without silica nanoparticles are shown. With the addition of silica nanoparticles at low concentrations, the solubility parameter is increased due to the increased Brownian motion; the difference between the solubility parameters of acetic acid and acetone is decreased, and the two liquids are mixed together easier. However, at higher concentrations of silica nanoparticles, the solubility parameters are decreased due to aggregation, and the difference between solubility parameters is

Table 3
Prediction of solubility parameter of toluene at presence of silica nanoparticles at 298 K and 1 atm.

vol% SiO_2	Wt. % SiO_2	Molecule SiO_2	Molecule Toluene	δ_t^{sim} $(J/cm^3)^{0.5}$	$\lvert\delta_{t\ Acetone}^{sim}-\delta_{t.solvent}^{sim}\rvert$	$\lvert\delta_{t\ Acetic\ Acid}^{sim}-\delta_{t.solvent}^{sim}\rvert$
0	0	0	500	18.556	1.806	2.647
0.028898	0.088275	1	738	19.204	1.158	1.999
0.037945	0.115888	1	562	19.702	0.659	1.501
0.062338	0.190293	1	342	19.789	0.572	1.414
0.100054	0.30519	1	213	18.662	1.699	2.541
1.018158	3.048192	23	477	18.436	1.926	2.767

Table 4
Prediction of solubility parameter of benzene at presence of silica nanoparticles at 298 K and 1 atm.

vol% SiO_2	Wt. % SiO_2	Molecule SiO_2	Molecule Benzene	δ_t^{sim} $(J/cm^3)^{0.5}$	$\lvert\delta_{t\ Acetone}^{sim} - \delta_{t.solvent}^{sim}\rvert$	$\lvert\delta_{t\ Acetic\ Acid}^{sim} - \delta_{t.solvent}^{sim}\rvert$
0	0	0	500	18.073	2.289	3.13
0.029167	0.08813	1	872	20.789	0.428	0.414
0.038185	0.115358	1	666	20.765	0.403	0.438
0.062469	0.188629	1	407	20.772	0.410	0.431
0.10006	0.301909	1	254	18.076	2.286	3.127
0.994936	2.948717	19	481	17.978	2.384	3.225

Table 5
Prediction of solubility parameter of carbon tetrachloride, n-butanol and n-butyl acetate at presence of silica nanoparticles at 298 K and 1 atm.

vol% SiO_2	Wt. % SiO_2	Molecule SiO_2	Molecule CCl_4	Molecule n-butanol	Molecule n-butyl acetate	δ_t^{sim} (J/cm3)$^{0.5}$	$\lvert\delta_{t\ Acetone}^{sim} - \delta_{t.solvent}^{sim}\rvert$	$\lvert\delta_{t\ Acetic\ Acid}^{sim} - \delta_{t.solvent}^{sim}\rvert$
0	0	0	500	–	–	17.916	2.44	3.287
			–	500	–	22.804	2.442	1.601
			–	–	500	18.549	1.813	2.654
0.029225	0.048799	1	455	–	–	19.124	1.238	2.079
0.029368	0.09527	1	–	850	–	22.270	1.908	1.067
0.029368	0.088185	1	–	–	586	19.183	1.178	2.02
0.038324	0.06399	1	397			17.659	2.674	3.515
0.038102	0.124547	1	–	650	–	22.617	2.255	1.414
0.038411	0.115317	1	–	–	448	18.631	1.731	2.572
0.062325	0.104048	1	324			18.875	1.507	2.328
0.063003	0.205827	1	–	393	–	22.767	2.405	1.564
0.062333	0.187047	1	–	–	276	18.597	1.765	2.606
0.100271	0.167353	1	233	–	–	18.83	1.528	2.373
0.100206	0.327091	1	–	247	–	22.626	2.264	1.423
0.100569	0.301554	1	–	–	171	18.963	1.399	2.24
1.8346	3.0268	37	463	–	–	17.965	2.397	3.238
0.916755	2.938076	18	–	482	–	22.318	1.956	1.115
1.01088	2.976902	28	–	–	472	18.320	2.042	2.883

increased. This trend is continued in a way that at concentrations over 3 wt%, the difference between the solubility parameter of benzene, toluene, n-butyl acetate solvents and acetic acid, acetone is increased to a value, which is even higher than the difference of pure solvents. According to the results of Forster et al. [42], and Greenhalgh et al. [41] research's on the deviation of solubility parameters of different compounds, all the solvents present in Tables 3–5 are miscible with acetic acid and acetone with silica nanoparticles concentration of 0.1 vol%. However, according to Tables 3–5, the best solvent for acetone is benzene with silica concentration of 0.038 vol%, and the best solvent for acetic acid is also benzene at silica concentration of 0.029 vol%. The difference of solubility parameters of benzene with acetic acid and acetone at silica nanoparticle concentrations of 0.038 vol% and 0.029 vol% is 0.403 $(J/cm^3)^{0.5}$ and 0.414 $(J/cm^3)^{0.5}$, respectively.

Considering the obtained results, the best solvents for acetone from top to bottom are benzene (0.038 vol%), toluene (0.062 vol%), n-butyl acetate (0.029 vol%), carbon tetrachloride (0.029 vol%), and n-butanol (0.029 vol%). The best solvents for acetic acid, in order, are benzene (0.029 vol%), n-butanol (0.029 vol%), toluene (0.062 vol%), n-butyl acetate (0.029 vol%), and carbon tetrachloride (0.029 vol%). In Fig. 4, plot of solubility parameters of solvents with respect to the volume concentration of silica

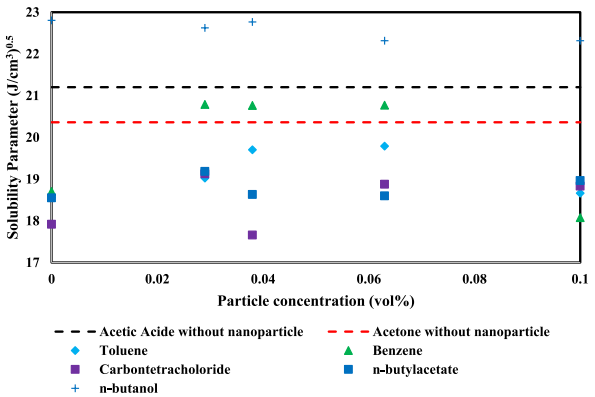

Fig. 4. Predicted solvents solubility parameters versus volume concentration of silica nanoparticles.

nanoparticles is drawn. In this plot, red and black dashed lines represent the solubility parameter of pure acetic acid and acetone, respectively, which are obtained from molecular dynamic simulation. According to this plot, the closer the solubility parameter of solvent is to the solubility parameter of acetone (red dashed line), and acetic acid (black dashed line), the more soluble that solvent is in acetic acid and acetone. Moreover, it can be deducted from the plot that only in the case of benzene and n-butanol, the solubility parameter is higher than the pure acetone in the presence of nanoparticles compared to the pure solvent, while for the acetic acid, all the solvents except n-butanol have lower solubility parameter with the presence of nanoparticles.

Table 6 shows the density, boiling point, melting point, and viscosity of toluene, benzene, carbon tetrachloride, n-butanol, and n-butyl acetate. Apart from closeness of solubility parameters, low melting point and viscosity, and high boiling point are the other characteristics of a good solvent. Considering the lower viscosity of toluene compared to n-butanol, and also due to the low difference between the boiling point of n-butanol (117.7 °C) and acetic acid (117.9 °C) [1], toluene is a better solvent than n-butanol for extraction of acetic acid from water. As a result, according to the data presented in Tables 3–6 and Fig. 4, for extraction of acetone and acetic acid from water, benzene solvent with silica nanoparticles concentrations of 0.038 vol%, and 0.029 vol%, respectively; and toluene solvent, both with nanoparticles concentration of 0.062 vol% are the best choices.

3.3. The effect of number of molecules (cell size) on the solubility parameter

In Fig. 5, the dependence of solubility parameter on the number of molecules in the simulation cell is shown. Here, only the results related to the solubility parameter of carbon tetrachloride is discussed, as the other solvents have similar behavior. In the simulation of this part, three systems with 250, 500, and 750 carbon tetrachloride molecules having the box length of 17.717, 17.916, and 17.844 Å, respectively, were constructed. The calculated solubility parameter for these simulation boxes were 17.717, 17.916, 17.844 $(J/cm^3)^{0.5}$, which are very close to the experimental value (17.8 $(J/cm^3)^{0.5}$) [46].

According to what can be seen in Fig. 5, the deviation between simulated solubility parameter and the experimental value (purple dashed line) is not very considerable and indicates the negligible effect of number of molecules on the results of the simulation. However, since the speed of the simulation with 500 molecules is about 1.86 times the speed with 750 molecules, 500 molecules were used also for the simulation of other compounds. Zhao et al. [51] reached the same conclusion as well for the effect of simulation box size on the diffusion coefficient of CO_2 in water, when comparing the results from three simulation boxes with the size of 30, 50, and 70 Å.

In Fig. 6, the effect of number of molecules (or cell size) on the solubility parameter of carbon tetrachloride with silica nanoparticles was investigated at the concentration of 0.072 %, and cell sizes of 37.4, 47.1, and 53.9 Å, containing $324CCl_4+1SiO_2$, $648CCL_4+2SiO_2$, and $648CCL_4+2SiO_2$ molecules, respectively, which showed the same results as the case without nanoparticles. However, because in this part, the density of solvents are different for toluene, benzene, carbon tetrachloride, n-butanol, and n-butyl acetate; for concentrations below 0.1 %, one silica nanoparticle molecule was used.

3.4. Binary mixtures

Miscibility of two compound is related to the formation of hydrogen bonds, difference in polarity, and dielectric constants [34]. Low difference in dielectric constants in polar liquids, favors the miscibility. In this section, the solubility or non-solubility of acetic acid and acetone at toluene, benzene, carbon tetrachloride, n-butanol, and n-butyl acetate solvents were studied by drawing the plot of relative concentration variation at z direction of amorphous cell. In the last section (prediction of solubility parameter), it was understood that acetic acid and acetone are soluble in the five solvents mentioned. Since the results of the simulation are heavily dependent on the parameters of the force field [52], if COMPASS force field is chosen, the relative concentration in the z direction should remain constant.

In Tables 7 and 8, the number of molecules in the simulation, weight percentage, simulation cell size, density of the cell at the end of simulation, calculated density from Aspen HYSYS software (at 298 K and 1 atm), and density experimental are shown. A total number of 500 molecules were used to construct each amorphous cell. In this step, the duration needed to reach equilibrium in the simulation with isothermal-isobaric ensemble (NPT) is considered 500 ps [52]. Moreover, Ewald summation method with precision of 0.01 kcal/mol was used for calculation of electrostatic interactions and Atom based summation method was used for calculation of van der Waals interactions with cut-off distance of 12.5 Å. Also, Velocity scale thermostat and Berendsen thermostat were utilized in all the simulations. The density of mixtures or pure compounds were obtained using NPT ensemble, which were very close to the values obtained from Aspen HYSYS software (simulation values were higher compared to the HYSYS values). According to the prior studies, calculated densities are systematically bigger than the experimental values [52–54].

Table 6
Density, boiling point, melting point, and viscosity of solvents.

	Density (g/cm^3)	Boiling point (°C)	Melting point (°C)	Viscosity (cP)
Toluene	0.867	110.6	−95	0.590 (20 °C)
Benzene	0.8765	80.1	5.5	0.6076 (25 °C)
n-butyl acetate	0.882	116.16	−78	0.685 (25 °C)
n-butanol	0.8058	117.7	−89.8	2.620 (25 °C)
Carbontetracholoride	1.5867	76.72	−23	0.86 (25 °C)

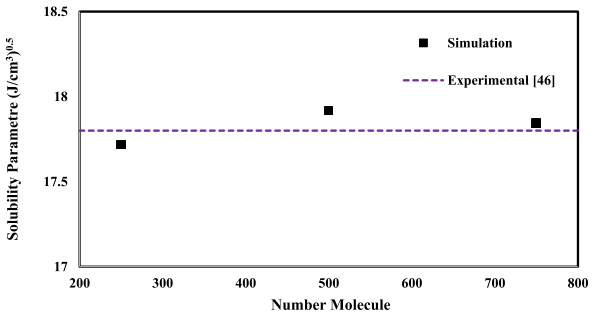

Fig. 5. The effect of number of molecules on the solubility parameter of pure carbon tetrachloride at 1 atm and 298 K.

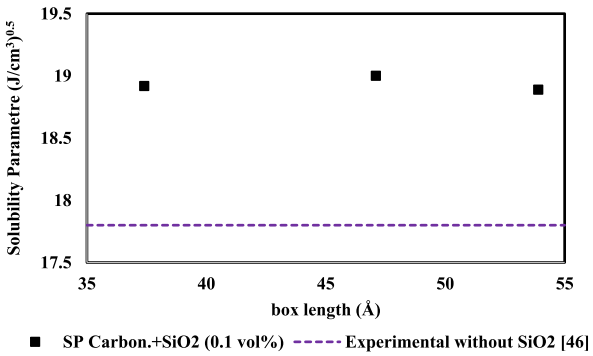

Fig. 6. The effect of number of molecules on the solubility parameter of carbon tetrachloride with 0.072 vol% of silica nanoparticles at 1 atm and 298 K.

Table 7
The number of molecules, weight percentage, density, and dimensions of amorphous cell for the binary mixture at 298 K and 1 atm.

Component	Number of molecules	Weight %	Density Exp (g/cm^3)	Density MD (g/cm^3)	Density HYSYS (g/cm^3)	a $\times b \times c$ (Å)
Acetone	250	38.7	0.83245	0.838	0.8349	35.3 × 35.3 × 60
Toluene	250	61.3				
Acetone	250	42.6	–	0.839	0.8298	33.7 × 33.7× 60
Benzene	250	57.4				
Acetone	250	27.4	–	1.247	1.238	34.4 × 34.4× 60
Carbon tetrachloride	250	72.6				
Acetone	250	43.9	0.8026	0.7889	0.8012	32.8 × 32.8× 60
n-butanol	250	56.1				
Acetone	250	33.3	0.8435	0.848	0.8478	37.7 × 37.7× 60
n-butyl acetate	250	66.7				

Table 8
The number of molecules, weight percentage, density, and dimensions of amorphous cell for the binary mixture at 298 K and 1 atm.

Component	Number of molecules	Weight %	Density Exp (g/cm^3)	Density MD (g/cm^3)	Density HYSYS (g/cm^3)	a $\times b \times c$ (Å)
Acetic Acid	250	39.5	0.918	0.9491	0.9164	39.8 × 39.8× 60
Toluene	250	60.5				
Acetic Acid	250	43.5	–	0.9513	0.9223	37.9 × 37.9× 60
Benzene	250	56.5				
Acetic Acid	250	28.1	–	1.41	1.3593	38.7 × 38.7× 60
Carbon tetrachloride	250	71.9				
Acetic Acid	250	44.8	0.9056	0.8945	0.9182	38.0 × 38.0 × 60
n-butanol	250	55.2				
Acetic Acid	250	34.1	0.9262	0.9538	0.9215	43.6 × 43.6 × 60
n-butyl acetate	250	65.9				

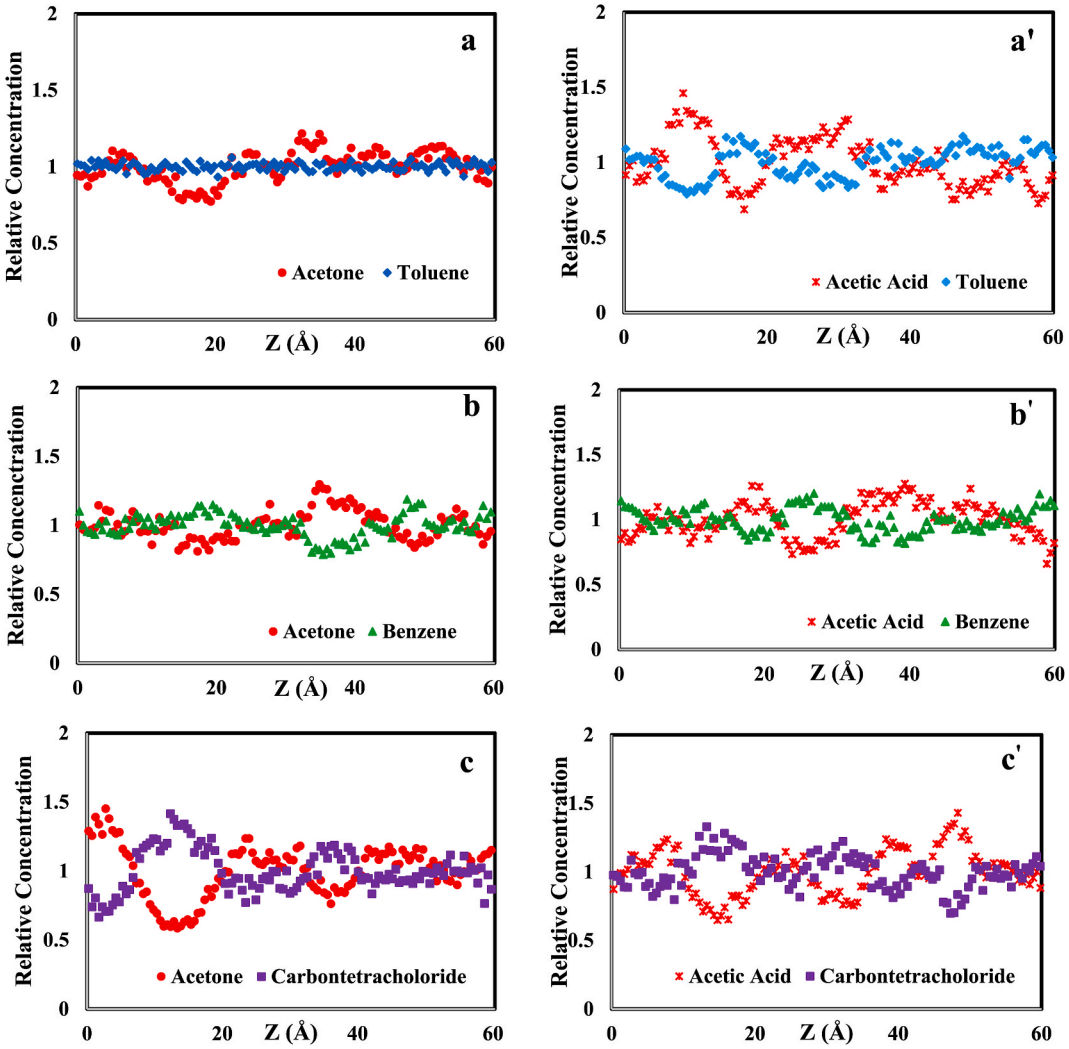

Fig. 7. Variation of relative concentration of binary mixture in the z direction of amorphous cell, the right column is for acetic acid and the left column is for acetone: a) toluene, b) benzene, c) carbon tetrachloride, d) n-butanol, e) n-butyl acetate at 298 K, 1 atm.

In Fig. 7, the variation of relative concentration of acetic acid and acetone binary mixture at five solvents of toluene (a), benzene (b), carbon tetrachloride (c), n-butanol (d), and n-butyl acetate (e) in the z-axis direction is plotted. As can be seen in Fig. 7(a–e), the plots of relative concentration of the binary mixtures are straight lines, which indicate the homogeneous distribution of compounds in the mixture and miscibility of binary mixtures. Moreover, according to the results obtained by Greenhalgh et al. [41], if the deviation of solubility parameter is less than 7 $(J/cm^3)^{0.5}$, the compounds are most certainly miscible. Since the deviation of solubility parameter of these solvents in the pure state is less than 7 $(J/cm^3)^{0.5}$, it can be concluded that acetic acid and acetone are soluble in all these solvents.

The dielectric constant of acetone and acetic acid are 20.7, and 6.2, and the dielectric constants of benzene, toluene, carbon tetrachloride, n-butanol, n-butyl acetate are equal to 2.25, 2.38, 2.23, 17.5, and 5.01, respectively. Since acetone has the properties of both polar and non-polar compounds, it is soluble in non-polar solvents due to the presence of two methyl groups. Moreover, acetic acid has polar and non-polar properties, too, and is soluble in non-polar solvent because of its methyl group. In a study carried out by Núñez-Rojas [52], on the extraction of benzene from dodecane using polar solvents and ionic liquids, by plotting benzene's density in the z direction, they figured out that benzene is soluble in polar solvents while dodecane is not soluble in these solvents.

In Table 9, the total number of molecules, weight percentage, dimensions of the simulation cells, density of the cell at the end of simulation, and the calculated density using Aspen HYSYS software for the binary mixture of water and other compounds at 298 K and 1 atm is shown. The weight percentages of the mixtures are almost equal. The total number of molecules in each cell was set to 500 molecules.

In Fig. 8, the variation of concentration in the binary mixture of water in seven compounds of acetone (a), acetic acid (b), toluene (c), benzene (d), carbon tetrachloride (e), n-butanol (f), and n-butyl acetate (g) in the z direction is plotted. Since water is polar, acetic

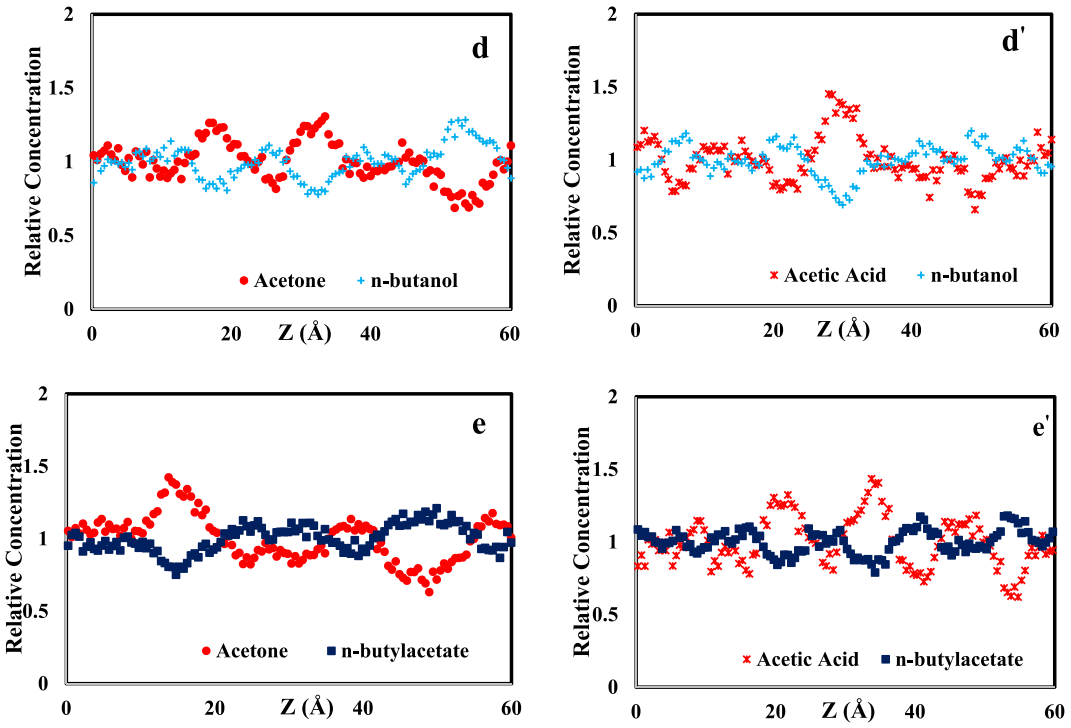

Fig. 7. (*continued*).

Table 9
The number of molecules, weight percentage, density, and dimensions of amorphous cell for the binary mixture.

Component	Number of molecules	Weight %	Density MD	Density HYSYS	a ×*b* × *c* (Å)
Water	382	50.1	0.891	0.8989	33.60 × 33.60× 33.60
Acetone	118	49.9			
Water	385	50.1	0.9767	1.022	28.47 × 28.47× 28.47
Acetic Acid	115	49.9			
Water	418	49.9	0.9328	0.9302	25.92 × 25.92× 40
Toluene	82	50.1			
Water	407	50.2	0.937	0.9352	25.43 × 25.43× 40
Benzene	93	49.8			
Water	448	50.2	1.294	1.229	22.7 × 22.7× 40
Carbon tetrachloride	52	49.8			
Water	402	49.9	0.8567	0.9019	25.84 × 25.84× 40
n-butanol	98	50.1			
Water	433	50.1	0.94	0.9393	26.23 × 26.23× 40
n-butyl acetate	67	49.9			

acid and acetone are capable of forming hydrogen bonds with water molecules and thus are soluble in water (Fig. 8-a, 8-b). It can be seen from Fig. 8-(c-g) that none of the compounds are soluble in water. This point can also be understood from the fact that the differences between the solubility parameter of water and other compounds is high (Table 2). Also, there is a considerable difference between the dielectric constant of water (the dielectric constant of water is 80) and non-polar solvents of toluene, benzene, carbon tetrachloride, n-butanol, and n-butyl acetate, which is in the favor of non-solubility.

4. Conclusion

Molecular dynamics simulation was utilized for the selection of best solvent for extraction of acetic acid and acetone from water. In the simulations, solvents with three inter-surface tension level of low, medium, and high (toluene, benzene, n-butyl acetate, carbon tetrachloride, and n-butanol) were used. The results of calculated solubility parameters and binary mixtures revealed that COMPASS force field can predict the solubility parameter of compounds in the presence or absence of nanoparticles with great accuracy. The simulations showed that by increasing the temperature, the solubility parameter would decrease. Furthermore, it was observed by calculation of carbon tetrachloride solubility parameter in three different cell dimensions (with and without the presence of

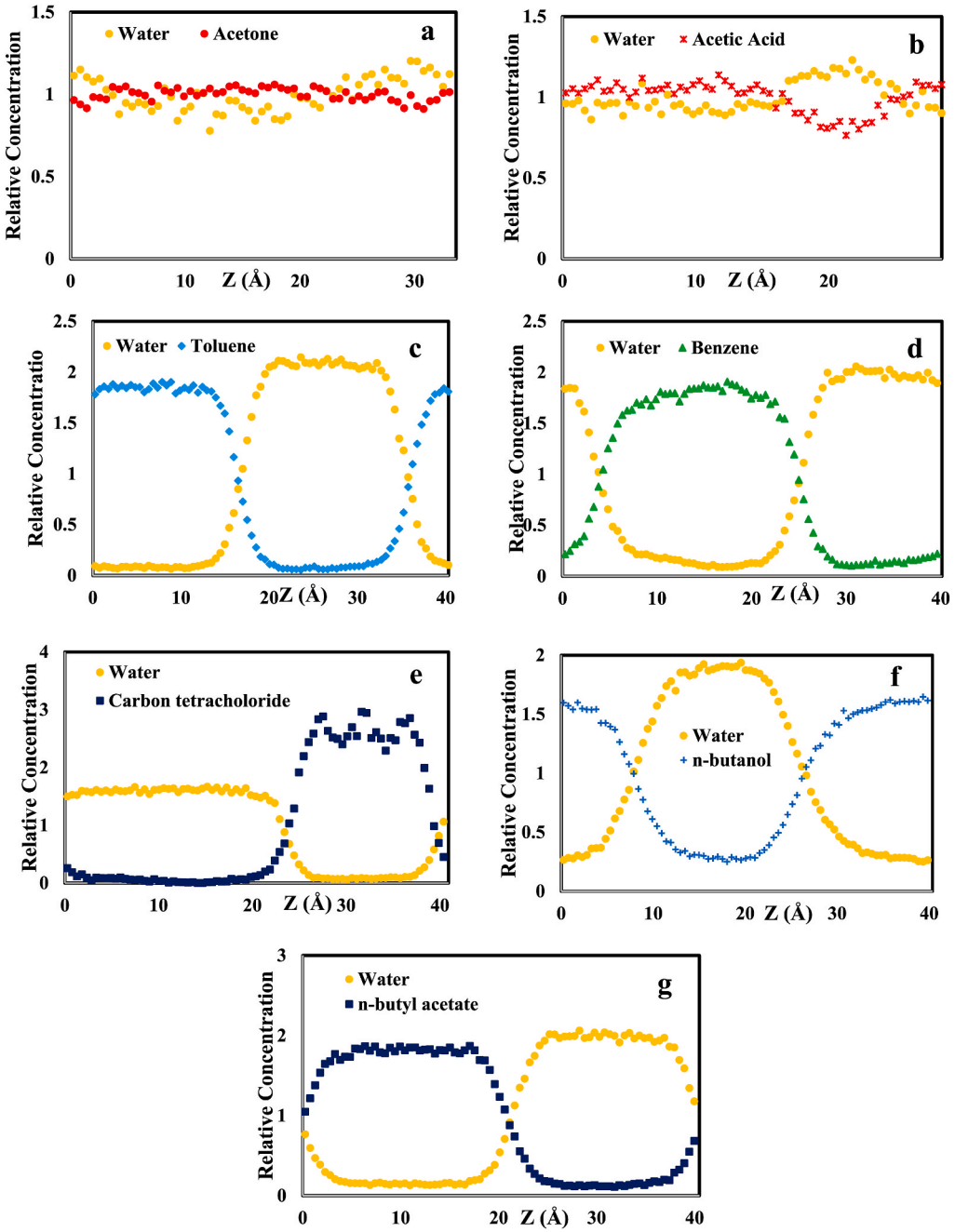

Fig. 8. Plot of relative concentration variation of binary mixture in the z direction of the amorphous cell: a) water-acetone, b) water-acetic acid, c) water-toluene d) water-benzene, e) water-carbon tetrachloride, f) water-n-butanol, and g) water-n-butyl acetate.

nanoparticles) that the size of the simulation cell (number of molecules) does not affect the solubility parameter. By studying the solubility parameter and the plot of relative concentration of binary mixtures, it was predicted that the best solvents for acetic acid and acetone are benzene (with 0.029 vol% and 0.038 vol%) and toluene (0.062 vol%), respectively. The results of solubility parameter showed that at low concentrations, increasing nanoparticles will increase the solubility parameter due to the increased Brownian motion. At higher concentrations, the solubility parameter started to decrease due to the aggregation, leading to a lower solubility parameter than the pure solvent at concentrations higher than 3 wt%.

Data availability

Data will be made available on request.

CRediT authorship contribution statement

Hojatollah Moradi: Writing – original draft, Validation, Software, Investigation, Data curation. **Hossein Bahmanyar:** Writing – review & editing, Supervision, Project administration, Conceptualization. **Hedayat Azizpour:** Writing – review & editing, Supervision, Project administration, Conceptualization.

Declaration of competing interest

The authors declare that they have no known competing financial interests or personal relationships that could have appeared to influence the work reported in this paper.

References

[1] L. Feng, et al., Liquid–liquid equilibrium study for the ternary system of Water+ acetic Acid+ 2-octanol, J. Chem. Eng. Data 65 (4) (2020) 1531–1537.
[2] Y. Wang, et al., Screening of imidazole ionic liquids for separating the acetone–n-hexane azeotrope by COSMO-SAC simulations and experimental verification, ACS Sustain. Chem. Eng. 8 (11) (2020) 4440–4450.
[3] Z. Huanhuan, et al., A review on recovery technologies of acetic acid from industrial wastewater, Chem. Ind. Eng. Prog. 34 (6) (2015) 1768.
[4] A. Warade, et al., Simulation of multistage countercurrent liquid-liquid extraction, Leonardo J. Sci. 20 (2011) 79–94.
[5] P. Amani, et al., A critical review on the use of nanoparticles in liquid–liquid extraction, Chem. Eng. Sci. 183 (2018) 148–176.
[6] W.L. McCabe, J.C. Smith, P. Harriott, Unit Operations of Chemical Engineering, McGraw Hill, Boston, 2001.
[7] T.J. Afolabi, T.I. Edewor, Liquid-liquid equilibrium data for butan-2-ol-ethanol-water, pentan-1-ol-ethanol-water and toluene-acetone-water systems, Int. J. Civ. Mech. Eng. 5 (12) (2011) 1124–1127.
[8] F. Kollerup, A.J. Daugulis, Ethanol production by extractive fermentation–solvent identification and prototype development, Can. J. Chem. Eng. 64 (4) (1986) 598–606.
[9] I. Akartuna, et al., Stabilization of oil-in-water emulsions by colloidal particles modified with short amphiphiles, Langmuir 24 (14) (2008) 7161–7168.
[10] G. Nematbakhsh, A. Rahbar-Kelishami, The effect of size and concentration of nanoparticles on the mass transfer coefficients in irregular packed liquid–liquid extraction columns, Chem. Eng. Commun. 202 (11) (2015) 1493–1501.
[11] M. Bahiraei, Particle migration in nanofluids: a critical review, Int. J. Therm. Sci. 109 (2016) 90–113.
[12] M. Amani, et al., Modeling and optimization of thermal conductivity and viscosity of $MnFe_2O_4$ nanofluid under magnetic field using an ANN, Sci. Rep. 7 (1) (2017) 1–13.
[13] S.P. Jang, S.U. Choi, Role of Brownian motion in the enhanced thermal conductivity of nanofluids, Appl. Phys. Lett. 84 (21) (2004) 4316–4318.
[14] J.H. Hildebrand, Solubility, J. Am. Chem. Soc. 38 (8) (1916) 1452–1473.
[15] G. Scatchard, Equilibria in non-electrolyte solutions in relation to the vapor pressures and densities of the components, Chem. Rev. 8 (2) (1931) 321–333.
[16] C. Li, A. Strachan, Cohesive energy density and solubility parameter evolution during the curing of thermoset, Polymer 135 (2018) 162–170.
[17] C.M. Hansen, The Three Dimensional Solubility Parameter, 1967, p. 14. Danish Technical: Copenhagen.
[18] H. Moradi, et al., Enhancement of supercritical carbon dioxide solubility models using molecular simulation data, Kor. J. Chem. Eng. 39 (3) (2022) 717–723.
[19] J. Chen, et al., New insights into the quantitative relationship between surface chemistry of fullerene (C60) and solubility parameters and compatibility with polymers, J. Phys. Chem. B 125 (20) (2021) 5420–5433.
[20] A.P.r. de la Luz, et al., A new force field of formamide and the effect of the dielectric constant on miscibility, J. Chem. Theor. Comput. 11 (6) (2015) 2792–2800.
[21] H. Moradi, et al., Prediction of methane diffusion coefficient in water using molecular dynamics simulation, Heliyon 6 (11) (2020) e05385.
[22] H. Moradi, et al., Molecular dynamics simulation of H2S adsorption behavior on the surface of activated carbon, Inorg. Chem. Commun. 118 (2020) 108048.
[23] H. Moradi, et al., Molecular dynamic simulation of carbon dioxide, methane, and nitrogen adsorption on Faujasite zeolite, Chin. J. Chem. Eng. 43 (2022) 70–76.
[24] H. Moradi, et al., Effect of Si/Al ratio in the faujasite structure on adsorption of methane and nitrogen: a molecular dynamics study, Chem. Eng. Technol. 44 (7) (2021) 1221–1226.
[25] M. Emamian, et al., Performance of molecular dynamics simulation for predicting of solvation free energy of neutral solutes in methanol, Chem. Prod. Process Model. 17 (5) (2022) 489–497.
[26] M. Moradi, H. Azizpour, M. Mohammarehnezhad-Rabieh, Determination of diffusion coefficient of C_2H_6 and CO_2 in hydrocarbon solvents by molecular dynamics simulation, J. Mol. Liq. 370 (2023) 121015.
[27] H. Moradi, H. Azizpour, M. Mohammadi, Study of adsorption of propane and propylene on CHA zeolite in different Si/Al ratios using molecular dynamics simulation, Powder Technol. (2023) 118329.
[28] M. Zhang, et al., Study on the solubility parameter of supercritical carbon dioxide system by molecular dynamics simulation, J. Mol. Liq. 248 (2017) 322–329.
[29] Y. Du, et al., *Molecular dynamics Study on the suitable compatibility Conditions of a CO_2-cosolvent-light hydrocarbon System by Calculating the solubility parameters*, Energy Fuel. 34 (3) (2020) 3483–3492.
[30] A. Marciniak, The solubility parameters of ionic liquids, Int. J. Mol. Sci. 11 (5) (2010) 1973–1990.
[31] A. Marciniak, The Hildebrand solubility parameters of ionic liquids—part 2, Int. J. Mol. Sci. 12 (6) (2011) 3553–3575.
[32] J. Gupta, et al., Prediction of solubility parameters and miscibility of pharmaceutical compounds by molecular dynamics simulations, J. Phys. Chem. B 115 (9) (2011) 2014–2023.
[33] D. Camper, et al., Gas solubilities in room-temperature ionic liquids, Ind. Eng. Chem. Res. 43 (12) (2004) 3049–3054.
[34] A. Finotello, et al., Room-temperature ionic liquids: temperature dependence of gas solubility selectivity, Ind. Eng. Chem. Res. 47 (10) (2008) 3453–3459.
[35] K. Paduszyński, et al., Liquid–liquid phase equilibrium of (piperidinium-based ionic liquid+ an alcohol) binary systems and modelling with NRHB and PCP-SAFT, Fluid Phase Equil. 305 (1) (2011) 43–52.
[36] P. Scovazzo, et al., Regular solution theory and CO_2 gas solubility in room-temperature ionic liquids, Ind. Eng. Chem. Res. 43 (21) (2004) 6855–6860.
[37] E.J. Maginn, Molecular simulation of ionic liquids: current status and future opportunities, J. Phys. Condens. Matter 21 (37) (2009) 373101.
[38] J. Hildebrand, R. Scott, Solutions of nonelectrolytes, Annu. Rev. Phys. Chem. 1 (1) (1950) 75–92.
[39] C.M. Hansen, Hansen Solubility Parameters: a User's Handbook, CRC press, 2007.
[40] M.A. Mohammad, A. Alhalaweh, S.P. Velaga, Hansen solubility parameter as a tool to predict cocrystal formation, Int. J. Pharm. 407 (1–2) (2011) 63–71.
[41] D.J. Greenhalgh, et al., Solubility parameters as predictors of miscibility in solid dispersions, J. Pharmaceut. Sci. 88 (11) (1999) 1182–1190.
[42] A. Forster, et al., Selection of excipients for melt extrusion with two poorly water-soluble drugs by solubility parameter calculation and thermal analysis, Int. J. Pharm. 226 (1–2) (2001) 147–161.

[43] M. Günther, et al., Hydrophilic solutes in modified carbon dioxide extraction—prediction of the extractability using molecular dynamic simulation, Eur. J. Pharmaceut. Sci. 25 (2–3) (2005) 321–329.
[44] Y.S. Sistla, L. Jain, A. Khanna, Validation and prediction of solubility parameters of ionic liquids for CO_2 capture, Separ. Purif. Technol. 97 (2012) 51–64.
[45] Y. Tong, et al., Thermodynamic analysis and molecular dynamic simulation of the solubility of saccharin in three binary solvent mixtures, J. Chem. Therm. 141 (2020) 105952.
[46] J. Burke, Solubility Parameters: Theory and Application, 1984.
[47] A. Bahmanyar, et al., Mass transfer from nanofluid drops in a pulsed liquid–liquid extraction column, Chem. Eng. Res. Des. 92 (11) (2014) 2313–2323.
[48] S. Rouina, et al., Investigating the effect of nanoparticles on the dispersed phase mass transfer coefficient in a rotary disc column, Chem. Eng. Process: Process Intensif. 104 (2016) 84–93.
[49] J. Saien, R. Hasani, Hydrodynamics and mass transfer characteristics of circulating single drops with effect of different size nanoparticles, Separ. Purif. Technol. 175 (2017) 298–304.
[50] C. Mochizuki, J. Nakamura, M. Nakamura, Development of non-porous silica nanoparticles towards cancer photo-theranostics, Biomedicines 9 (1) (2021) 73.
[51] X. Zhao, H. Jin, Correlation for self-diffusion coefficients of H_2, CH_4, CO, O_2 and CO_2 in supercritical water from molecular dynamics simulation, Appl. Therm. Eng. 171 (2020) 114941.
[52] E. Núñez-Rojas, H.M. Flores-Ruiz, J. Alejandre, Molecular dynamics simulations to separate benzene from hydrocarbons using polar and ionic liquid solvents, J. Mol. Liq. 249 (2018) 591–599.
[53] E.J. González, B.a. González, E.n.A. Macedo, Thermophysical properties of the pure ionic liquid 1-butyl-1-methylpyrrolidinium dicyanamide and its binary mixtures with alcohols, J. Chem. Eng. Data 58 (6) (2013) 1440–1448.
[54] M.P. Singh, et al., Viscoelastic, surface, and volumetric properties of ionic liquids [BMIM], J. Chem. Eng. Data 59 (8) (2014) 2349–2359 *[$OcSO_4$],[BMIM][PF_6], and [EMIM][MeSO3]*.